

**This accepted author manuscript is copyrighted and published by Elsevier. It is posted here by agreement between Elsevier and MTA. The definitive version of the text was subsequently published in European Polymer Journal, 74, 2016, DOI: 10.1016/j.eurpolymj.2015.11.028 Available under license CC-BY-NC-ND.**

# Corona-electrospinning: needleless method for high-throughput continuous nanofiber production

*Kolos MOLNAR<sup>1,2</sup>, Zsombor K. NAGY<sup>3\*</sup>*

<sup>1</sup> Department of Polymer Engineering, Faculty of Mechanical Engineering, Budapest University of Technology and Economics, Műegyetem rkp. 3-9. H-1111, Budapest, Hungary

<sup>2</sup> MTA–BME Research Group for Composite Science and Technology, Műegyetem rkp. 3., H-1111, Budapest, Hungary

<sup>3</sup> Department of Organic Chemistry and Technology, Faculty of Chemical Technology and Biotechnology, Budapest University of Technology and Economics, Budafoki út 8, H-1111, Budapest, Hungary

\* corresponding author, email: [zsknagy@oct.bme.hu](mailto:zsknagy@oct.bme.hu); tel: +36 1 4631424; fax:+36 1 463 3648

**Keywords:** Electrospinning, polymer nanofibers, corona-electrospinning, high-output spinneret, scale-up, industrialization

**Abstract.** A novel spinneret and modified electrospinning method is introduced where with nanofibers can be produced with high-throughput. The main conception of the system is to continuously supply the polymeric solution through a narrow, but long gutter bounded by a metal electrode having sharp edge. As there is no high free liquid surface volatile and low boiling point solvents can be applied that makes the method suitable for pharmaceutical and biomedical applications. In this study the operation of the spinneret was tested with polyacrylonitrile/dimethyl-formamide and poly-vinylpyrrolidone/ethanol solutions. The charge concentration – related from the construction - was investigated by finite element analysis. The highest electrical charge density is formed along the sharp edge what results many self-assembled Taylor-cones that is also confirmed by the first operation experiences. The productivity of the technique can be two orders of magnitude higher than that of the single capillary method.

## **Introduction**

Electrospinning has gained a high interest in the last years as it is a simple method for generating nanofibers. The process can be commercially feasible, as there are currently companies which produce nanofiber mats and nowadays application of these can even be realized in filtration masks or HEPA filters, protective or military clothing, etc. [1]. It is a promising technology especially in the pharmaceutical industry based on price and performance analysis. Electrospun nanofibers have unique advantages for dissolution enhancement of drugs with poor water solubility (e.g. high specific surface area, complete amorphization, formation of solid solution, providing supersaturation, better wettability, [2,3]). However, the applications of electrospun nanofibers in this field are in just the early development phase. Probably, one of the main obstacles of industrial development and commercialization of electrospun material-based

pharmaceutical formulations is the challenging scale-up of the technology and to comply with the strict standards.

At classical electrospinning the fibers are formed by electrostatic forces, instead of mechanical ones. Both the main advantage and disadvantage of the technology is that fiber formation and deposition happens in the same time and space, resulting in a nanofibrous mat with quasi-random fiber orientation [4,5]. The technique is therefore efficient as having one technology step, forming nanofibers and fiber structure in a top-down process. Preparation of special fiber structures is possible using coaxial [6], triaxial [7] or side-by-side [8] electrospinning techniques. There are also special setups making possible to form oriented and aligned structures [9-11], nanofiber yarns [12-16], coated [17] and 3D structures [15], etc.

Although electrospinning technique itself is quite simple, it is still a big challenge to increase the productivity of the process [18]. One capillary typically has an output between 0.1 and 5 ml/h, depending on solvent, polymer and different additives. The produced fibers typically have a mass flow one order of magnitude smaller as the solvent has to be evaporated [4].

The simplest way to increase the productivity of electrospinning is the multiplication of the needles. Their number can reach thousands and the productivity can be increased significantly, however cleaning of such a spinneret is rather difficult and clogging of the needles can cause serious solution feeding and spinning problems [19, 20]. Electrospinning can be implemented by using capillary holes instead, leading to a simpler construction, but the same fiber formation and maintenance problems occur [21].

The emerged difficulties related to the needles can be avoided by using needleless electrospinning methods. Electrospinning from a free liquid surface without using needle is possible if the gradient of the electric field is high enough at the liquid surface therefore the jet

forming forces and stresses can overcome the surface tension of the solution. Several types of needleless fiber spinnerets have been developed for increasing the productivity of nanofiber manufacturing. Conductive magnetic particles [22] or cylinders [23,24], discs [25], wires [26], balls [27] can be agitated or rotated in a polymer solution and many self-organized Taylor-cones can be formed from the surface of them which can result in high throughput production. Conducting gas into a polymer solution to achieve bubble electrospinning [28-31] is also capable to increase the production rate of nanofibers. Lu et al. [32] used a conductive rotary cone as a spinneret together with a glass pipe as a feeder for high throughput electrospinning. The glass pipe directed the polymer solution to the outer part of the charged rotating cone and Taylor-cones were formed at the bottom edge of the spinneret. The main challenge which emerges concerning this technique is the controllability of the polymer solution supply at the edge. Thoppey et al. [33, 34] have recently described a similar method which is bowl-based and called edge electrospinning. A fluid-filled bowl was used both as a polymer solution container and as a spinneret. The reported technique is a promising scale-up approach of electrostatic spinning, however it is a batch method and continuous production of nanofibers would be preferred from industrialization aspects.

All things considered, the main drawback of the mentioned needleless methods is the occurrence of a relatively large free liquid surface (at polymer solution container and/or at rotating cone taper) where besides jet formation other, undesired processes can take place such as water vapor absorption, solvent evaporation and in extreme cases ignition due to corona discharge, too.

Concentration and composition change of the polymer solution due to solvent evaporation or water vapor absorption can cause serious negative effects on the electrospinning process. Thicker fibers, solid material at the spinneret (beards) or unsolidified material on the collector can occur especially in case of long-term production, thus the avoidance of excessive evaporation and water

vapor absorption is required to develop an industrially feasible electrospinning process. In industrial scales it is also important to keep a low solvent concentration in the electrospinning space. The ventilation leads to even more significant changes in the solution having a considerable free surface.

Water vapor absorption can be minimalized by controlling the humidity of air, however the avoidance of excessive evaporation when a volatile solvent is used (e.g. tetrahydrofuran (THF), dichloromethane (DCM), ethanol, methanol, acetone, etc.) seems complicated if a relatively large free liquid surface is present for evaporation. Probably, that is why mainly solvents with high boiling point (e.g. water, DMF) were used in the earlier-mentioned publications partly because of the application of volatile solvents which seems incompatible with the presented needleless electrospinning techniques due to the presence of relatively large free liquid surface. On the other hand the reason why solvents with low boiling point are predominantly used in pharmaceutical formulation is their easier removability resulting in << under the limit >> residual solvent content in the product which might be crucial for solvents with higher boiling points (e.g. DMF).

Thus the aim was to develop an electrospinning method which is capable for high-throughput production of nanofibers and suitable to use volatile solvents in order to meet the requirements of the pharmaceutical industry. The novel technology offers continuous operation with high-throughput and a simple, easy-to-maintain needleless spinneret construction operating with minimized free liquid surface hence minimizing the solvent evaporation. In this paper the new electrospinning method and related results with a volatile (ethanol) and a less volatile (DMF) solvent are introduced.

### ***3. Materials and methods***

### 3.1. Approach

A novel electrospinning method and spinneret was developed and patented [35] by the authors. The main conception of the spinning system is to continuously supply the polymeric solution through a narrow, but long circular-shaped gutter bounded by a metal electrode ring having sharp edge (the *corona*). The highest electrical charge density is formed along the sharp edge what results many self-assembled Taylor-cones. The spinneret is rotated amongst the symmetry line in order to homogeneously disperse the polymer solution amongst the circular gutter hence preventing the local overflow of the solution. The spinneret, with appropriate bearings and sealing, is rotated with adjustable, but moderate speed. The solution is continuously supplied through a fixed hollow shaft in the center. Fibers are collected on a nonwoven textile having continuous traction speed. A schematic drawing of the procedure can be seen in Figure 1.

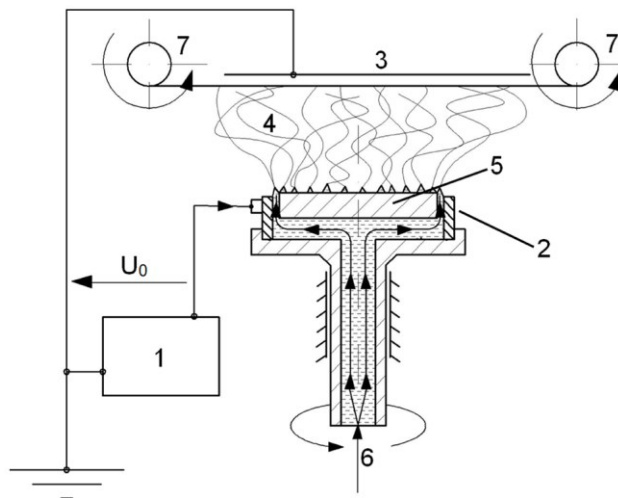


Figure 1. Schematic figure of the electrospinning setup equipped with the novel spinneret. 1: high voltage power supply, 2: circular electrode having sharp edge, 3: grounded collector screen, 4: fiber formation space, 5: lid, 6: solution feed, 7: traction of the collector textile [35]

### 3.2. Applied materials

In this study two different materials were studied to demonstrate the operation of the new spinneret and related technology. To study the electrospinning process with a volatile solvent PVPK30 (BASF) type poly-vinylpyrrolidone was dissolved in ethanol to make a 20 wt% concentrated solution. In our former studies [36, 37] we gained a lot of experience with polyacrylonitrile (PAN) therefore we used it as a second model material of the process. Filament fibers acquired from a carbon fiber manufacturing company (wished to remain anonymous) were dissolved in dimethyl-formamide (DMF, Aldrich) to create a 12 wt% solution. This solution concentration was optimal for single-needle electrospinning based on our former results.

### **3.3. Electrospinning parameters**

In this study the operation of the novel spinneret was compared to that of the classical, single-capillary electrospinning method, where a single, hypodermic needle with an inner diameter of 0.7 mm was applied. The *corona*-spinneret was tested in two different constructions, a smaller one made mainly by rapid prototyping and a bigger, improved prototype that was a machined aluminum construction. The sharpened electrode's (Figure 1. 2.) diameter was 42 mm and 110 mm respectively.

MA2000 NT 65/P (Hungary) type high voltage power supply was used for the experiments. The applied voltage, the distance between the grounded metal electrode and the *corona*-spinneret was set to 55 kV and 120 mm, respectively. Solutions were fed by Aitecs SEP-10S plus (Lithuania) syringe pump with the maximum flow rate which produced permanent fiber formation without overflow. The attainable flow rate was tested by continuous fiber formation and stable operation

for at least 2 hours. The rotation speed of the spinneret was 90 rpm. The nanofibers were collected on a polypropylene nonwoven substrate with a constant traction speed of 100 mm/min. From this textile the nanofibers could be easily peeled off.

The prototype of the electrospinning device equipped with the aluminum *corona*-spinneret can be seen in Figure 2. The electrospinning process was going continuously for hours. Compared to other technologies using free liquid surface, there is no liquid reservoir and a small amount of solution (approximately 5 ml) is enough to start the process. The solution can be fed continuously through the process.

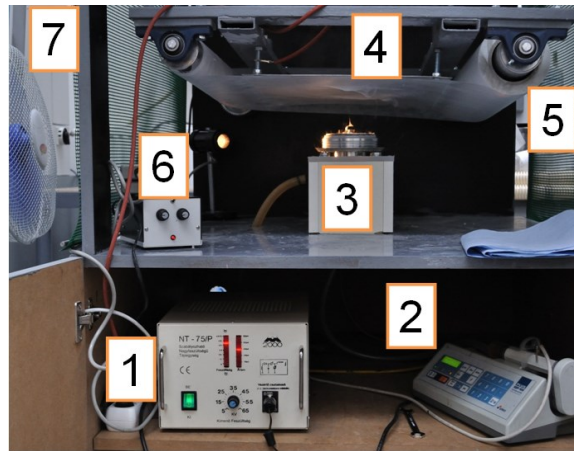


Figure 2. The *corona*-electrospinning setup 1: power supply, 2: solution feed, 3: corona-spinneret, 4: collector and substrate textile, 5: traction rolls, 6: speed control, 7: fan for ventilation

### 3.4. Image processing

Scanning electron microscopy (SEM) was carried out on the produced nanofiber mats by JEOL 6380 LA (Japan) device. The surface of the samples was coated by JEOL JFC-1200 fine coater with fine gold-palladium (Au-Pd) alloy layer in order to avoid their charging. The determination



of the average diameter was performed by using UTHSCSA Image Tool 3.0 type image processing software.

### **3.5. Finite element analysis**

Finite element analysis (FEA) was carried out by Ansys FEA software in order to get a detailed view on the electric field distribution of the classical and the self-developed methods. The results of the local electric field intensities of different methods were compared.

## **4. Results and discussion**

### **4.1. Finite element analysis of the processes**

In order to compare the single needle and corona-electrospinning finite element analysis (FEA) was carried out. The geometry of our first prototype spinneret and the conventional single needle was applied, respectively for the simulation. As boundary conditions the upper part of the stainless steel collector electrode was grounded and the electrode of the same material was charged to high voltage. The other parts of the corona spinneret are made of (and modeled by) insulating plastics and besides that air is present in the fiber forming space. All the conditions (collector-spinneret distance, size of collector, etc.) was set according to the nanofiber production experiments, and in order to investigate the forming electrostatic field the applied voltage was set to a step of 1 kV in both cases. The results of the electric field analysis can be seen in Figure 3.

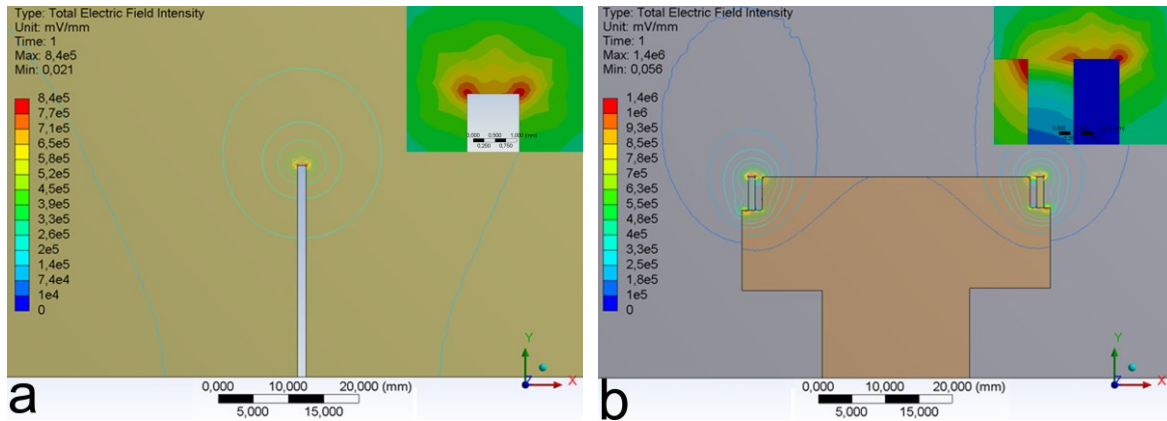


Figure 3. FEA of the electrostatic field intensity. a) single capillary setup, b) corona electrospinning (both figures including detailed view).

It can be seen that there is a charge concentration at the sharp tip/edge of the spinneret. This charge concentration leads to a high local field strength that enhances the formation of Taylor-cones. Figure 4. also represents the results of the finite element analysis, but in this case the lines indicate the intersection of the electrical equipotential surfaces with the observation plane. At the single needle setup the electric field encompasses the whole needle. The highest gradient is in vertical direction just to the direction of the collector electrode, at the tip of the needle that helps the fiber formation. At corona electrospinning the lines are even denser along the metal electrode of the spinneret. The gradient of the electric voltage is slightly differs from vertical resulting in diverging forming fibers. That leads to a higher area of fiber deposition i.e. if the fiber deposition radius of the single capillary is extended with the diameter of the corona spinneret that is still a smaller size than the corona spinneret produces. In the case of corona-electrospinning technology, the direction of the local gradient of the electric field can be set by geometry hence modifying the divergence of fibers in the initial, exiting zone.

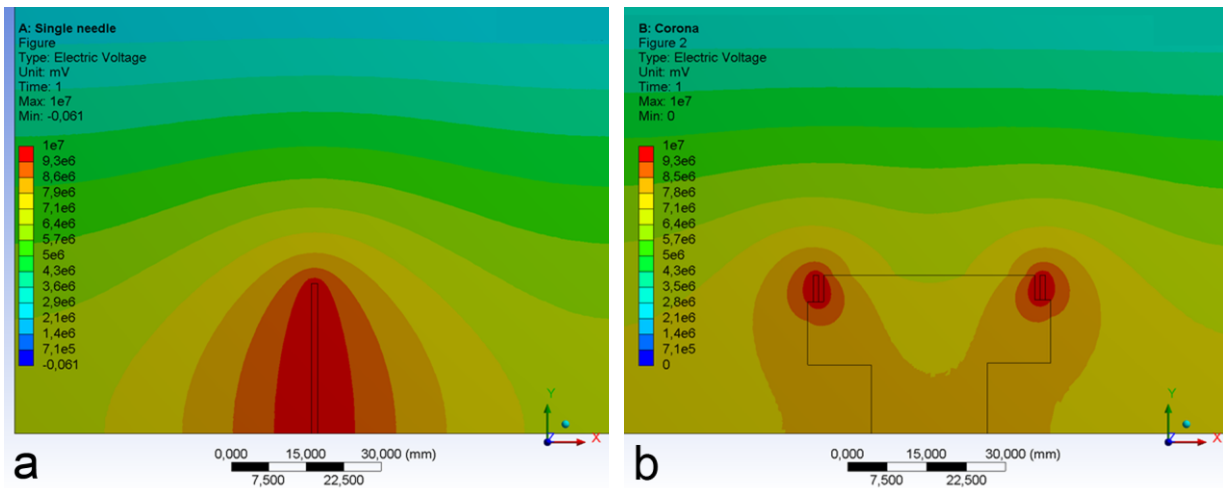


Figure 4. FEA of the voltage distribution a) single needle electrospinning, b) *corona*-electrospinning

#### 4.1. Experiments with PVP

The Taylor-cone formation during the process can be seen in Figure 5. for both the small, rapid prototyping-made ( $d_1 = 42$  mm) and the bigger aluminum ( $d_2 = 110$  mm) prototype spinnerets. Even distribution of the forming nanofibers can be observed along the edge of the charged electrode.

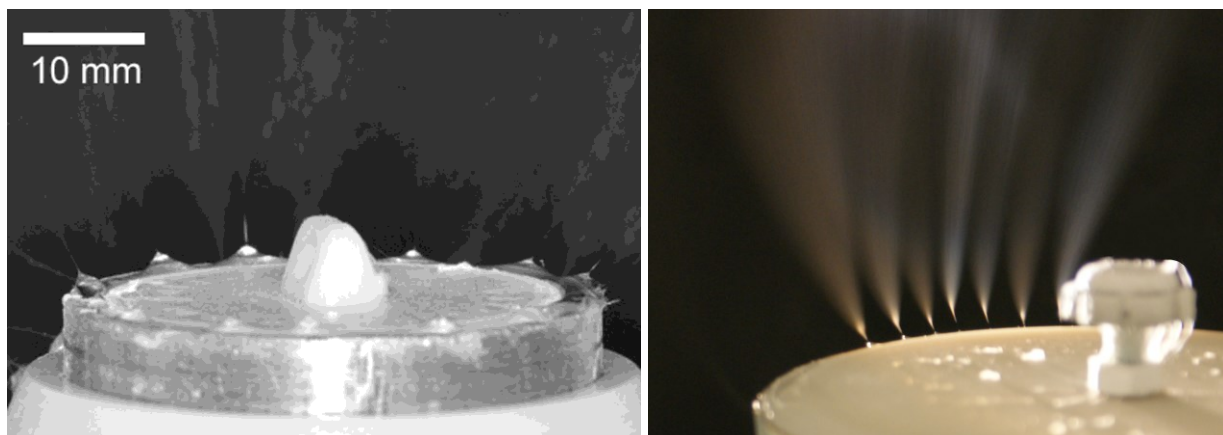


Figure 5. Taylor-cone formation along the round metal electrode of the spinneret a) 42 mm diameter, b) 100 mm diameter

The corona-electrospinning resulted in higher throughput compared to that of the single-needle setup. With the smaller, 42 mm diameter electrode the feed rate could reach 120 ml/h without overflowing; while at single-needle setup only 8 ml/h could be reached. With the bigger (110 mm) setup 300 ml/h could be set where intense ventilation was necessary to remove the evaporating solvent from the electrospinning space. *Corona*-electrospinning requires higher voltage, as fiber formation began at around 30 kV, while with the single-needle setup the initial voltage was around 15 kV. SEM images of the fibers can be seen in Figure 6. The average fiber diameter was 550 nm at *corona*-electrospinning (spun at 55 kV) and 530 nm at single needle electrospinning (at 25 kV). However higher field strength is formed in case of *corona*-electrospinning the small difference is formed that can be originated from the different solvent evaporation conditions (i.e. earlier solidification of the fibers) caused by ventilation.

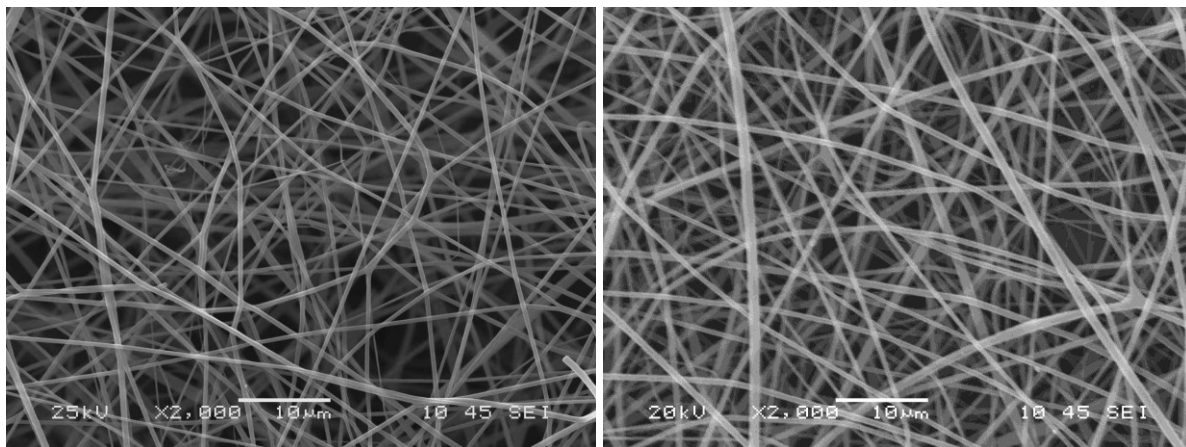


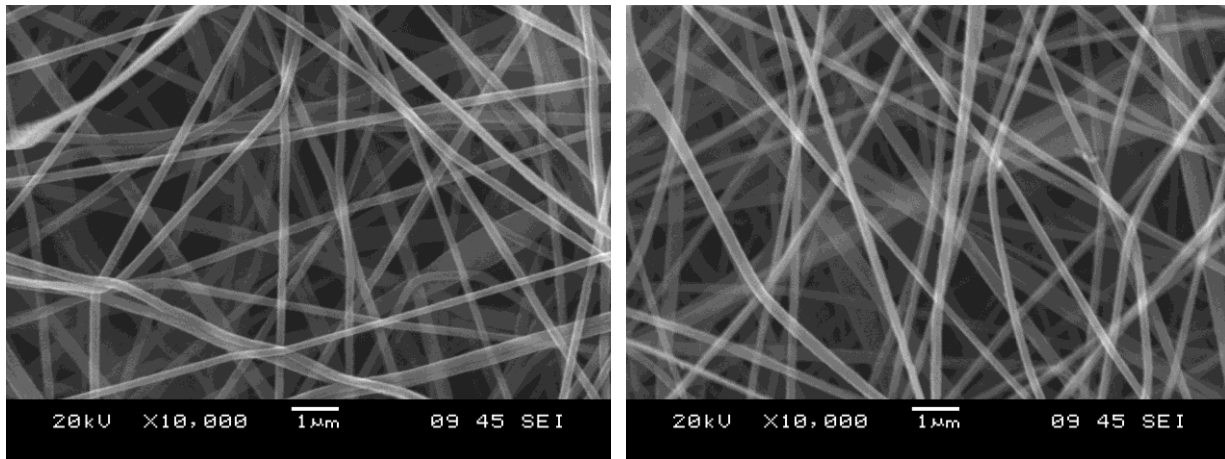
Figure 6. SEM images of the obtained PVP nanofibers produced by A) single capillary electrospinning, B) *corona*-electrospinning

## 4.2. Experiments with PAN

The 110 mm diameter *corona-spinneret* showed highly-increased productivity compared to that of the single-capillary setup. With the PAN-DMF material the continuous flow rate reached 60 ml/h while the rate of the capillary setup was only 3 ml/h. The nanofibers were deposited in an approximately 280 mm wide continuous stripe. From the spinneret-collector distance, the diameter of the spinneret and the deposition characteristics it could be calculated that the fibers are scattered and diverged within  $37^\circ$  angle from vertical travel direction due to the repulsion of the parallel formed jets and electrospinning instabilities. That also fits well to our expectations based on the FEA model (Figure 4.). It is assumed that the fibers would travel perpendicular to the direction of the equipotential lines (i.e. to the direction of more sudden color change). As a first approximation this gradient vector points approximately in the direction where fibers are formed and deposited. Geometrical considerations and experimental observations shows that in the case of single capillary setup this fiber deposition region is smaller; the related deposition scattering angle is estimated to be  $15^\circ$  only (that is the angle of the half cone of fiber formation space).

The jet formation required approximately 20 kV in the case of single capillary and 40 kV in the case of corona-electrospinning. By increasing the voltage to 25 kV and 55 kV, respectively, the processes became more stable and effective. In the case of *corona*-electrospinning the number of jets was counted and it was found to be  $176 \pm 16$  / m relative to the edge length of the metal electrode. In such sense the process acts like having capillaries arranged in every 5-6 mm.

Besides the productivity, the morphology of fibers is also an important standard of quality. The SEM images of the PAN nanofibers can be seen in Figure 7.



A)

B)

Figure 7. SEM images of the nanofibers produced by A) single capillary electrospinning, B) *corona-electrospinning*

The fiber diameter distributions can be seen in Figure 8. The average fiber diameter (and its deviation) was  $214 \text{ nm} \pm 68 \text{ nm}$  in the case of single capillary, and  $187 \text{ nm} \pm 65 \text{ nm}$  in the case of *corona-electrospinning* that is 15% smaller. It can be explained by the results of the FEA analysis. Higher local electric field is formed close to the spinneret, where the material is yet unsolidified (Figure 3.). Compared to the former case with ethanol in this case the solvent evaporation is slower making possible to generate thinner fibers.

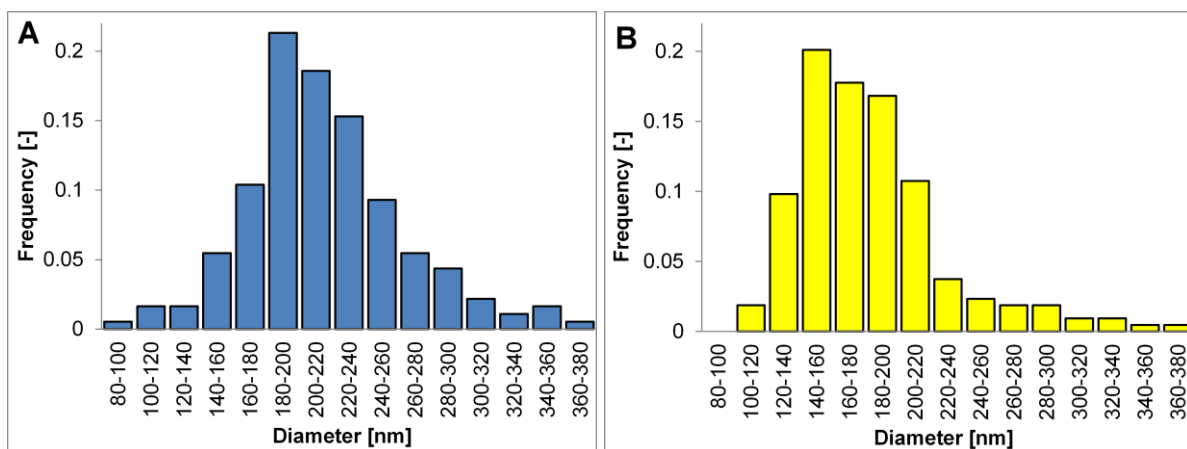


Figure 8. Fiber diameter distributions of PAN nanofibers. A) single capillary setup, B) *corona*-electrospinning method

## 5. Conclusions

The novel approach makes possible to produce nanofibers by high throughput with a simple construction spinneret. The method is efficient as the applied electrode is a sharp edge that concentrates charges exactly at the location where Taylor-cones are formed which was confirmed by FEA simulations. As there is no high free liquid surface volatile and low boiling point solvents can be applied. The operation of the new spinneret and the method was demonstrated at PAN dissolved in DMF, and at PVP dissolved in ethanol. The diameter and morphology of the resulted nanofibers are close to those which were processed by the classical setup. The rotation of the spinneret made possible to avoid the overflow of the electrospinning solution and led to higher flow rates. A small size prototype made possible a 20-50 time increase in productivity compared to the single capillary method. The density of forming Taylor-cones is in the magnitude of 100-200/m depending on the material, the construction type and spinneret size [19]; however detailed description needs further research. In the future it is planned to determine the optimal distance between the round-shaped electrode and the lid and the optimal construction of the spinneret in order to further develop and exploit the promising preliminary results.

## Acknowledgements

This research was supported by the Hungarian Research Fund (OTKA K100949, PD108975, PD116122) and the János Bolyai Research Scholarship of the Hungarian Academy of Sciences. This work is connected to the scientific program of the “Development of quality-oriented and

harmonized R+D+I strategy and functional model at BME” project. This project is supported by the New Széchenyi Plan (Project ID: TÁMOP-4.2.1/B-09/KMR-2010-0002).

## References

1. Persano L., Camposeo A., Tekmen C., Pisignano D., Industrial upscaling of electrospinning and applications of polymer nanofibers: a review. *Macromolecular Materials and Engineering* 298, 504-520 (2013).
2. Nagy Z.K., Balogh A., Vajna B., Farkas A., Patyi G., Kramarics Á., Marosi G., Comparison of electrospun and extruded soluplus-based solid dosage forms of improved dissolution. *Journal of pharmaceutical sciences* 101, 322-332 (2012)
3. Agarwal S., Wendorff J.H., Greiner A., Use of electrospinning technique for biomedical applications. *Polymer*, 49, 5603-5621 (2008).
4. Andradý A.L.. *Science and Technology of Polymer Nanofibers*. John Wiley & Sons, Inc., New Jersey (2008).
5. Reneker D.H., Yarin A.L., Electrospinning jets and polymer nanofibers. *Polymer*, 49, 2387-2425 (2008).
6. Yu D.G., White K., Chatterton N., Li Y., Li L., Wang X., Structural lipid nanoparticles self-assembled from electrospun core-shell polymeric nanocomposites. *RSC Advances*, 5, 9462-9466 (2015) DOI: 10.1039/C4RA14001J
7. Yu D.G., Li X.Y., Wang X., Yang J.H., Bligh A., Williams G.R., Nanofibers fabricated using triaxial electrospinning as zero order drug delivery systems *ACS Appl. Mater. Interfaces*, 7, 18891–18897 (2015) DOI: 10.1021/acsami.5b06007
8. Chen G., Xu Y., Yu D.Y., Zhang D.F., Chatterton N.P., White K.N., Structure-tunable Janus fibers fabricated using spinnerets with varying port angles. *Chemical Communications*, 51, 4623-3626, (2015) DOI: 10.1039/C5CC00378D
9. Lee C.H., Shin H.J., Cho I.H., Kang Y.M., Kim I.A., Park K.D., Shin J.W., Nanofiber alignment and direction of mechanical strain affect the ECM production of human ACL



- fibroblast, *Biomaterials*, 26, 11, 1261-1270 (2005),  
<http://dx.doi.org/10.1016/j.biomaterials.2004.04.037>.
10. Rakesh G.R., Ranjit G.S., Karthikeyan K.K., Radhakrishnan P., Biji P., A facile route for controlled alignment of carbon nanotube-reinforced, electrospun nanofibers using slotted collector plates. *eXPRESS Polymer Letters*, 9, 105–118 (2015).  
DOI: 10.3144/expresspolymlett.2015.12
  11. Yang Y., Wimpenny I., Ahearne M., Portable nanofiber meshes dictate cell orientation throughout three-dimensional hydrogels, *Nanomedicine: Nanotechnology, Biology and Medicine*, 7, 131-136 (2011).  
<http://dx.doi.org/10.1016/j.nano.2010.12.011>.
  12. Shao-Hua Wu, Xiao-Hong Qin, Uniaxially aligned polyacrylonitrile nanofiber yarns prepared by a novel modified electrospinning method, *Materials Letters*, 106, 204-207,  
<http://dx.doi.org/10.1016/j.matlet.2013.05.010>.
  13. Xuefen Wang, Kai Zhang, Meifang Zhu, Hao Yu, Zhe Zhou, Yanmo Chen, Benjamin S. Hsiao, Continuous polymer nanofiber yarns prepared by self-bundling electrospinning method, *Polymer*, 49, 11, 2755-2761 (2008).  
<http://dx.doi.org/10.1016/j.polymer.2008.04.015>.
  14. Mohamed Basel Bazbouz, George K Stylios, Novel mechanism for spinning continuous twisted composite nanofiber yarns, *European Polymer Journal*, 44, 1, 1-12 (2008),  
<http://dx.doi.org/10.1016/j.eurpolymj.2007.10.006>.
  15. B. Sun, Y.Z. Long, H.D. Zhang, M.M. Li, J.L. Duvail, X.Y. Jiang, H.L. Yin, Advances in three-dimensional nanofibrous macrostructures via electrospinning, *Progress in Polymer Science*, 39, 5, 862-890 (2014).  
<http://dx.doi.org/10.1016/j.progpolymsci.2013.06.002>.
  16. Eugene Smit, Ulrich Büttner, Ronald D. Sanderson, Continuous yarns from electrospun fibers, *Polymer*, 46, 8, 2419-2423 (2005),  
<http://dx.doi.org/10.1016/j.polymer.2005.02.002>.
  17. Jian-Xin He, Yu-Man Zhou, Yan-Chao Wu, Rang-Tong Liu, Nanofiber coated hybrid yarn fabricated by novel electrospinning-airflow twisting method, *Surface and Coatings Technology*, 258, 2014, 398-404, <http://dx.doi.org/10.1016/j.surfcoat.2014.08.062>.

18. Nagy Z.K., Wagner I., Suhajda Á., Tobak T., Harasztos A.H., Vigh T., Sóti P.L., Pataki H., Molnár K., Marosi G., Nanofibrous solid dosage form of living bacteria prepared by electrospinning eXPRESS Polymer Letters, 8, 352–361(2014)  
DOI:10.3144/expresspolymlett.2014.39
19. Theron S.A., Yarin A.L., Zussmann E., Kroll E.: Multiple jets in electrospinning: experiment and modeling. Polymer 46, 2889-2899 (2006).
20. Kim G.H., Cho Y-S., Kim W.D.: Stability analysis for multi-jets electrospinning process modified with a cylindrical electrode. European Polymer Journal, 42, 2031-2038 (2006).
21. Varabhas J.S., Chase G.G., Reneker D.H.: Electrospun nanofibers from a porous hollow tube. Polymer, 49, 4226-4229 (2008).
22. Yarin A.L., Zussman E.: Upward needleless electrospinning of multiple nanofibers. Polymer, 45, 2977-2980 (2004).
23. Jirsák O, Sanetrnik F, Lukas D, Kotek V, Martinova L, Chaloupek J: A method of nanofibers production from a polymer solution using electrostatic spinning and a device for carrying out the method. US patent W02005024101 (2005).
24. Li J., Gao F., Liu L.Q., Zhang Z., Needleless electro-spun nanofibers used for filtration of small particles. eXPRESS Polymer Letters 7, 683–689 (2013).  
DOI: 10.3144/expresspolymlett.2013.65
25. Jentsch E., Gül Ö., Öznergiz E., A comprehensive electric field analysis of a multifunctional electrospinning platform, Journal of Electrostatics, 71, 294-298 (2013),  
<http://dx.doi.org/10.1016/j.elstat.2012.12.007>.
26. Keith M. Forward, Alexander Flores, Gregory C. Rutledge, Production of core/shell fibers by electrospinning from a free surface, Chemical Engineering Science, 104, 250-259 (2013),  
<http://dx.doi.org/10.1016/j.ces.2013.09.002>.
27. Niu, H., Wang, X., Lin, T.: Needleless electrospinning: influences of fibre generator geometry. Journal of the Textile Institute 103, 787-794 (2012).
28. Liu Y., He J-H.: Bubble electrospinning for mass production of nanofibers. International Journal of Nonlinear Sciences and Numerical Simulation, 8, 393-396 (2007).
29. Yang R., He J., Xu L., Yu J.: Bubble-electrospinning for fabrication nanofibers. Polymer 50, 5846-5850 (2009).

30. Smit E.A., Sanderson R.D.: Process for the fabrication of fibers, US patent 0207303 (2010).
31. Reneker D.H., Chase G.G., Sunthornvarabhas J.: Bubble launched electrospinning jets. US patent 0283189 (2010).
32. Lu, B., Wang, Y., Liu, Y., Duan, H., Zhou, J., Zhang, Z., Wang, Y., Li, X., Wang, W., Lan, W., Superhigh-Throughput Needleless Electrospinning Using a Rotary Cone as Spinneret. *Small* 6, 1612-1616 (2010).
33. Thoppey N.M., Bochinski J.R., Clarke L.I., Gorga R.E., Unconfined fluid electrospun into high quality nanofibers from a plate edge, *Polymer* 51, 2010, 4928-4936, <http://dx.doi.org/10.1016/j.polymer.2010.07.046>.
34. Thoppey N.M., Gorga R.E., Clarke L.I., Bochinski J.R., Control of the electric field–polymer solution interaction by utilizing ultra-conductive fluids, *Polymer*, 55 (24), 6390-6398 (2014). <http://dx.doi.org/10.1016/j.polymer.2014.10.007>.
35. Molnár K., Nagy Z.K., Marosi G., Mészáros L., Electrospinning spinneret and modified electrospinning method for producing nanofibers in productive ways. Hungarian patent appl. P1200677 Budapest, Hungary (2012).
36. Molnár K., Szolnoki B., Toldy A., Vas L.M., Thermochemical stabilization and analysis of continuously electrospun nanofibers - Carbon nanotube-loaded polyacrylonitrile nanofibers for high performance carbon nanofiber mass production. *Journal of Thermal Analysis and Calorimetry*, 117, 1123–1135 (2014).
37. Molnár K., Szabéni G., Szolnoki B., Marosi G., Vas L.M., Toldy A., Enhanced conductivity composites for aircraft applications: carbon nanotube inclusion both in epoxy matrix and in carbonized electrospun nanofibers. *Polymers for Advanced Technologies*, **25**, 981-988 (2014). DOI: 10.1002/pat.3339
38. Molnár K, Vas LM. Bhattacharyya D, Fakirov S, editors. Synthetic Polymer-Polymer Composites, Chapter 10: *Electrospun Composite Nanofibers and Polymer Composites*. München: Hanser, 2012. pp. 301-352.
39. Lukas D., Sarkar A., Pokorny P., Self-organization of jets in electrospinning from free liquid surface: A generalized approach. *Journal of Applied Physics*, 103, 084309 (2008) DOI: 10.1063/1.2907967